American Mineralogist, Volume 88, pages 1970–1978, 2003

Composition, $Fe^{3+}/\Sigma Fe$, and crystal structure of non-asbestiform and asbestiform amphiboles from Libby, Montana, U.S.A.

MICKEY E. GUNTER,[1,*] M. DARBY DYAR,[2] BRENDAN TWAMLEY,[3] FRANKLIN F. FOIT JR.,[4] AND SCOTT CORNELIUS[4]

[1]Department of Geological Sciences, University of Idaho, Moscow, Idaho 83844-3022, U.S.A.
[2]Department of Earth and Environment, Mount Holyoke College, South Hadley, Massachusetts 01075, U.S.A.
[3]University Research Office, University of Idaho, Moscow, Idaho 83844-3010, U.S.A.
[4]Department of Geology, Washington State University, Pullman, Washington 99164-2812, U.S.A.

ABSTRACT

Compositional data and $Fe^{3+}/\Sigma Fe$ ratios obtained by electron microprobe and Mössbauer analyses are given for a suite of three amphibole and amphibole-asbestos samples collected from the former vermiculite mine near Libby, Montana. A crystal structure analysis, compositional data, and $Fe^{3+}/\Sigma Fe$ values for two samples from a previous study are also reported. The results confirm the conclusion drawn in the previous study that these amphiboles are dominantly compositions ranging from winchite to richterite. Mössbauer spectroscopy yielded $Fe^{3+}/\Sigma Fe$ ratios from 58% to 72% for the five samples.

The crystal structure was determined for a single crystal selected from a bulk sample. Its formula (as determined by electron microprobe analysis and Mössbauer spectroscopy) is $(K_{0.19}Na_{0.32})_A(Na_{0.85}Ca_{1.12}Mn_{0.03})_B(Mn_{0.01}Mg_{4.43}Fe^{3+}_{0.34}Fe^{2+}_{0.19}Ti_{0.01}Al_{0.02})(Al_{0.03}Si_{7.97}O_{22})(OH_{1.63}F_{0.37})$. The refinement was carried out based on space group $C2/m$, with $a = 9.879(2)$, $b = 18.024(3)$, $c = 5.288(1)$ Å, $\beta = 104.377(3)°$ and using data collected at room temperature. Mg is partitioned among the M1, M2, and M3 sites. All of the Fe^{3+} occupies M2, while Fe^{2+} is split between M2 and M3; Ca and Na fill the M4 site, while Na and K occupy the partially filled A site. The A-site occupancy is calculated as 0.51 based on chemical data, but only 0.48 based on X-ray diffraction results. Minerals with the former values would be classified as richterite and those with the latter as winchite.

INTRODUCTION

National attention focused on the small town of Libby, Montana in November 1999 when a newspaper article in the Seattle Post-Intelligencer chronicled asbestos-related diseases found in local miners, with the asbestos contaminant suggested to be the amphibole mineral tremolite. Within days, the United States Environmental Protection Agency arrived in Libby and began an investigation and remediation effort; the area is now a Superfund site. These recent actions are connected to the now-closed vermiculite mine located near Libby. The mine operated from the 1920s until 1990 and had the world's largest vermiculite production; however, the vermiculite ore contained several percent amphibole, both asbestiform and non-asbestiform varieties (Gunter et al. 2001). In the mid 1980s, two independent research groups, one funded by W.R. Grace, owners of the mine (McDonald et al. 1986a, 1986b, 1988), and another funded by the National Institute for Occupational Safety and Health (Amandus and Wheeler 1987; Amandus et al. 1987a, 1987b) performed health studies and found elevated mortality rates from asbestosis, mesothelioma, and lung cancer in the former miners.

The vermiculite mine was located in a Cretaceous-age ultramafic igneous body composed of a series of ring dikes with a post-mining, near-circular exposure of about 3 km in diameter. The ultramafic complex is adjacent to and associated with a syenite body that intruded metamorphic rocks of Precambrian age. The intrusion is roughly concentric and consists of a biotitite core surrounded by biotite pyroxenite, which is in turn surrounded by a magnetite pyroxenite. (see Boettcher 1967 for a detailed discussion of the geology and a geologic map.) The biotite in the biotite pyroxenite was altered to vermiculite by low-temperature weathering, whereas the pyroxenes were altered to amphiboles under higher-temperature hydrothermal processes (Boettcher 1966). Most of the mining was in the biotite pyroxenite. After the vermiculite ore was mined and enriched, it was expanded by rapid heating to form the commercial product Zonolite, which was used in many consumer products such as absorbents, fireproofing materials, industrial fillers, packaging material, and soil amendments. Another of the major uses of Zonolite was in attic insulation. Recently, W.R. Grace estimated that this product is in 15 million homes in the United States. Unfortunately, Zonolite may contain traces of amphiboles and amphibole-asbestos up to 2.8 wt% (USEPA 2000). There is an ongoing debate about the possible health effects on the residents of these homes (USEPA 2001). For a more detailed overview of the mining, geology, mineralogy, and health studies, see Bandli (2002) and references therein.

In a previous study, Wylie and Verkouteren (2000) performed chemical analyses of two amphibole samples from the former mine site. They identified the samples as winchite and

* E-mail: mgunter@uidaho.edu

not, as reported numerous times, tremolite or actinolite (e.g., Amandus and Wheeler 1987; Amandus et al. 1987a, b; MacDonald et al. 1986a, 1986b, 1988; USEPA 2000). However, Wylie and Verkouteren (2000) did not report $Fe^{3+}/\Sigma Fe$ values or F analyses of their two samples. Nor had they personally collected either of the samples. The location of their sample no. 1 was not known, and the location of recently collected sample no. 2 was reported simply as "the mine dump." Not only were there several mine dumps at the former mine site, but the samples in the mine dump may have been from overburden and not from the mining area. In the present study, we analyzed both of their samples for $Fe^{3+}/\Sigma Fe$ and performed a crystal structure refinement of a single crystal of their sample no. 2. We also performed chemical analyses and determined $Fe^{3+}/\Sigma Fe$ values for three samples we collected in the biotite pyroxene zone of the mine.

Asbestos classification and amphibole species names

Regulatory agencies classify certain species of amphibole as asbestos when they occur in the asbestiform habit. These regulated species are riebeckite, cummingtonite-grunerite, anthophyllite, and actinolite-tremolite (USEPA 2000). Tremolite, for example, occurs in both a regulated asbestiform habit and non-regulated, non-asbestiform habit. It is a continuing challenge to appropriately apply the definition of asbestos, applicable to populations of fibers, to the counting of individual particles in samples. Only samples of the above-listed species of amphiboles are regulated as "asbestos." Other amphibole species, however, occur in asbestiform varieties, such as winchite (Wylie and Huggins 1980 and Table 1) and richterite (vein sample, Table 1). The amphibole "asbestos" occurring at Libby has proven to be very harmful (McDonald et al. 1986a, 1986b, 1988; Amandus and Wheeler 1987; Amandus et al. 1987a, 1987b), and it is now apparent that much of the amphibole at Libby is non-regulated winchite and richterite.

Amphibole nomenclature (i.e., the naming of species) is complex because of the variations in chemistry and the many substitutions that occur in this mineral group. Leake et al. (1997) divided amphiboles into four groups based on B-site occupancy, given the general formula $AB_2C_5T_8O_{22}(OH)_2$, as follows: (1) the magnesium–iron–manganese–lithium group, where $(Ca + Na)_B < 1.0$ and $(Mg + Fe + Mn + Li)_B \geq 1.0$; (2) the calcic group, where $(Ca + Na)_B \geq 1.0$ and $Na_B \leq 0.5$; (3) the sodic–calcic group, where $(Ca + Na)_B \geq 1.0$ and $0.5 < Na_B < 1.5$; and (4) the sodic group, where $Na_B \geq 1.5$. Approximately eighty species names were then classified in each of the four groups based on Si content, $Mg / (Mg + Fe^{2+})$ ratio, and more detailed subdivisions of both the A- and B-site occupancies. In the general formula used by Leake et al. (1997), "C" refers to the sum of the contents of the M1, M2, and M3 octahedral sites and B refers to the larger M4 octahedral site. Both winchite and richterite are sodic-calcic amphiboles [i.e., $(Ca + Na)_B \geq 1.0$ and $0.5 < Na_B < 1.5$], whereas tremolite is a calcic amphibole [i.e., $(Ca + Na)_B \geq 1.0$ and $Na_B \leq 0.5$]. The important point here is that a slight change in the B-site occupancy places these species into different groups. Winchite and richterite are distinguished from each other based on their A-site occupancy, with winchite having $(Na + K)_A < 0.5$ and richterite $(Na + K)_A \geq 0.5$.

Sample selection and data collection

Five samples were selected for this study, and two of these, WV no. 1 and WV no. 2, are the same specimens examined by Wylie and Verkouteren (2000). WV no. 1 had been collected "ten-years earlier" from an unknown location at the mine site, and WV no. 2 was recently collected from a "mine dump." Their locations and geological occurrences are unknown. Bulk samples from their study were used to determine $Fe^{3+}/\Sigma Fe$ by Mössbauer spectroscopy, and a single crystal from WV no. 2 was selected for structural and electron microprobe (EMPA) analysis. No new EMPA data were collected from WV no. 1.

M.E. Gunter collected three samples called "vein," "outcrop," and "float" in October 1999 from the biotite pyroxenite zone in the center of the former Libby vermiculite mine. These samples were chosen to represent the different modes of occurrence of the amphiboles observed at the mine. The vein sample came from an approximately 2 cm wide vein of cross-fiber amphibole cross-cutting the biotite pyroxenite. The outcrop sample was collected in place, on a former mined-out bench of biotite pyroxenite; the sample showed an intergrowth of pyroxenes and amphiboles, in which the amphiboles were apparent alteration products of the pyroxenes. The float sample, an approximately 2–3 kg boulder consisting almost entirely of amphibole, was collected in the same area. For all three of these samples, Mössbauer spectroscopy was performed on bulk samples to determine $Fe^{3+}/\Sigma Fe$, and EMPA was done on single particles to obtain a complete chemical analysis.

Experimental methods and results

Electron microprobe analysis (EMPA)

Several grains of the three Libby amphibole samples (vein, outcrop, and float) were dispersed in epoxy on three separate standard petrographic slides. The samples were an approximately 50–50 mixture of amphibole fibers and fragments (Gunter et al. 2001). Because of the friable nature of the particles and their small size (minimum width approximately 1 μm) much work was required to obtain a suitable polish. A similar preparation method was used for a single crystal from sample WV no. 2* (the "*"denotes this as the crystal used in the structure analysis). The amphiboles were analyzed in the GeoAnalytical Laboratory, Washington State University, using a Cameca Camebax electron microprobe employing wavelength dispersive spectrometry, acceleration voltages of 20 kV (for WV no. 2* and the vein sample) and 15 kV (for the other samples), a beam current of 12 nA, and a beam diameter of 2 μm. The lower accelerating voltage was used for most analyses because of the small grain sizes. A Phi(Rho-Z) absorption correction and conventional fluorescence and atomic number corrections were applied to all data.

Table 1 lists compositions of the samples used in this study. The data in the first two columns in Table 1 are taken from Wylie and Verkouteren (2000). Column three shows the composition of WV no. 2* and represents an average of 25 analyses collected from the single crystal. Listings for the vein, outcrop, and float samples represent an average of 16 analyses from eight separate crystals, one analysis of each of nine crystals, and one analysis of each of 16 crystals, respectively. The compositional variability within the single crystals in the vein sample is similar to the variability among the individual samples, so we chose to perform only one analysis per crystal. We noted no chemical variability as a function of morphology (i.e., fibers vs. fragments). Also listed in Table 1 are the $Fe^{3+}/\Sigma Fe$ ratios (to be discussed later). Chemical formulas were calculated based on 23 (O) for WV no. 1 and WV no. 2 and 24 (O, OH, F, Cl) for WV no. 2* and the three Libby samples we collected. Site assignments were made following the recommendations of Leake et al. (1997).

Mössbauer spectroscopy

Mössbauer spectroscopy studies of amphiboles date back to the original work by Bancroft and coworkers (Bancroft et al. 1967a, 1967b; Bancroft and

TABLE 1. Electron microprobe analyses for amphiboles in this study and the study by Wylie and Verkouteren (2000)

	WV no. 1	WV no. 2	WV no. 2*	Vein	Outcrop	Float
SiO_2	56.6(4)	56.4(2)	57.48(38)	57.10(27)	57.54(41)	57.45(64)
Al_2O_3	0.5(1)	0.4(1)	0.32(4)	0.14(3)	0.13(3)	0.19(10)
TiO_2	nd	nd	0.10(2)	0.11(8)	0.04(3)	0.12(10)
FeO†	2.54	1.49	1.63(5)	2.29(21)	1.97(30)	1.51(20)
Fe_2O_3	3.85	3.01	3.29(10)	4.63(43)	4.93(75)	4.40(60)
MgO	20.2(5)	21.0(4)	21.43(23)	20.19(38)	20.10(78)	20.83(48)
MnO	0.1(0)	0.3(3)	0.32(8)	0.47(6)	0.16(4)	0.09(3)
CaO	8.3(10)	8.8(2)	7.51(17)	6.04(70)	7.63(1.63)	8.07(84)
Na_2O	3.2(8)	3.4(2)	4.35(21)	4.93(49)	3.84(1.04)	3.67(43)
K_2O	0.7(1)	0.8(2)	1.08(5)	1.25(24)	0.93(26)	0.82(11)
H_2O (diff)	nd	nd	1.77(5)	1.82(14)	1.93(10)	1.99(8)
F	nd	nd	0.84(12)	0.68(28)	0.48(19)	0.34(14)
Total‡			99.76(45)	99.37(52)	99.47(53)	99.34(54)
$Fe^{3+}/\Sigma Fe$	57.7	64.5	64.5	64.5	69.3	72.4
FeO_{EMPA}	6.0(6)	4.2(4)	4.59(13)	6.46(59)	6.40(97)	5.47(74)
No. analyses	6	3	25	16	9	16
pfus	for 23O	for 23O	for 24O	for 24O	for 24O	for 24O
Si	7.98	7.95	7.97(3)	7.99(2)	8.01(4)	7.98(4)
Al	0.08	0.07	0.05(1)	0.02(0)	0.02(10)	0.03(2)
Ti	nd	nd	0.01(0)	0.01(1)	0.00(0)	0.01(1)
Fe^{2+}	0.30	0.18	0.19(1)	0.27(2)	0.23(4)	0.18(2)
Fe^{3+}	0.41	0.32	0.34(1)	0.49(4)	0.52(8)	0.46(6)
Mg	4.24	4.43	4.43(4)	4.21(8)	4.17(15)	4.32(9)
Mn	0.01	0.04	0.04(1)	0.06(1)	0.02(1)	0.01(0)
Ca	1.25	1.34	1.12(2)	0.91(10)	1.14(24)	1.20(13)
Na	0.87	0.93	1.17(6)	1.34(14)	1.04(29)	0.99(12)
K	0.13	0.14	0.19(1)	0.22(4)	0.17(5)	0.15(2)
H	nd	nd	1.63(5)	1.70(12)	1.79(9)	1.85(6)
F	nd	nd	0.37(5)	0.30(12)	0.21(9)	0.15(6)
Site occupancies						
T-Si	7.98	7.95	7.97	7.99	8.01	7.98
T-Al	0.02	0.05	0.03	0.01	–	0.02
T-Ti	–	–	–	–	–	–
Sum T	8.00	8.00	8.00	8.00	8.01	8.00
C-Al	0.06	0.02	0.02	0.01	0.02	0.01
C-Ti	–	–	0.01	0.01	0.00	0.01
C-Fe^{2+}	0.29	0.18	0.19	0.27	0.23	0.18
C-Fe^{3+}	0.41	0.32	0.34	0.49	0.52	0.46
C-Mg	4.24	4.43	4.43	4.21	4.17	4.32
C-Mn	–	0.04	0.01	0.01	0.02	0.01
Sum C	5.00	4.99	5.00	5.00	4.96	4.99
B-Fe^{2+}	0.01	–	–	–	–	
B-Mn	0.01	–	0.03	0.05	–	–
B-Ca	1.25	1.34	1.12	0.91	1.14	1.20
B-Na	0.73	0.66	0.85	1.04	0.86	0.80
Sum B	2.00	2.00	2.00	2.00	2.00	2.00
A-Na	0.14	0.27	0.32	0.30	0.18	0.19
A-K	0.13	0.14	0.19	0.22	0.17	0.15
Sum A	0.27	0.41	0.51	0.52	0.35	0.34

Note: All EMPA data are from this study, except values in columns 1 and 2, which are from Wylie and Verkouteren (2000).
* WV no. 2 remeasured in this study.
† FeO and Fe_2O_3 are recalculated from the EMPA FeO and the Mössbauer $Fe^{3+}/\Sigma Fe$. Cl was included in EMPA analyses on our samples but was below 0.01 pfus.
‡ Totals corrected for F.

Burns 1969; Bancroft and Brown 1975). Spectroscopists now follow the site assignments (Table 2) proposed by Goldman (1979). However, only limited work has been done on samples from the sodic-calcic subgroup of the amphiboles. Virgo (1972) reported the first spectra of richterite, followed by the work of Litvin et al. (1973) on taramite. Luys et al. (1983) reported spectra of "amosite," "crocidolite," and anthophyllite asbestos. Ghose et al. (1986) reported Mössbauer spectra of Mn-rich winchite, as did Nysten and Skogby (1994). Most recently, Schmidbauer et al. (2000) gave Mössbauer data for three calcic amphiboles, Sokolova et al. (2000) reported spectra of an unusual strontian potassic-richterite, and Sokolova et al. (2001) gave data for ferrian winchite similar to the one studied here. However, no one has taken advantage of recent advances in fitting Mössbauer spectra. Because there is no analytical solution for the transmission integral represented by a Mössbauer spectrum (Vanderberghe et al. 1994), various methods for simplifying the problem of fitting the spectra were proposed. These include fitting: (1) pure Lorentzian line shapes (as used in the studies just mentioned); (2) a Gaussian distribution of Lorentzian line shapes, known as a Voigt line shape (Voigt 1912); and (3) quadrupole splitting or hyperfine field distributions (Ping et al. 1991). To date, the first of these procedures is the only one to be commonly used worldwide because commercial software for the other two approaches has not been available until very recently.

The approach of fitting quadrupole splitting distributions (QSD) has been shown to be superior to the Lorentzian-based approach in spectra in which there are poorly resolved quadrupole pairs, as is the case in mica (and probably amphibole) spectra. The QSD approach works best in samples where the Fe atoms

TABLE 2. Quadrupole splittings for sodic and calcic amphiboles* (Adapted and updated from Goldman 1979)

Species	M1	M2	M3	M4	Citation
Tremolite-actinolite Fe^{2+}	2.80–2.90	1.70–1.90	2.20–2.60	n.a.	Burns and Greaves (1971)
Hornblende Fe^{2+}	2.79–2.84	2.01–2.09	2.59–2.70	1.70	Bancroft and Brown (1975) Goodman and Wilson (1976)
Magnesio-hastingsite Fe^{2+}	2.70	2.00	2.70	n.a.	Semet (1973)
Sodic amphiboles Fe^{2+}	2.80	2.00	2.40	n.a.	Bancroft and Burns (1969) Ernst and Wai (1970)
Calcic amphiboles Fe^{2+}	2.80 with M3	2.20	2.80 with M1	1.80	Goldman (1979)
Calcic amphiboles Fe^{2+}	2.61–2.79	2.21–2.50		1.80–1.91	Schmidbauer et al. (2000)
Sodic amphiboles Fe^{3+}		0.42–0.50			Ernst and Wai (1970)
Sr potassirichterite Fe^{3+}		0.67			Sokolova et al. (2000)
Ferrian winchite Fe^{3+}		0.48			Sokolova et al. (2001)

Note: n.a. = not analyzed or fitted.
*All quadrupole splittings are from room-temperature spectra and are presented in mm/s. Isomer shifts are not tabulated because they are constant, over a range from 1.10–1.15 mm/s for Fe^{2+} and 0.35–0.48 for Fe^{3+}.

are not surrounded by a perfectly homogeneous array of neighbors and next-nearest neighbors. Effectively, the QSD models the local distortions and atomic disorder surrounding the Fe atoms, rather than simply reflecting the ideal point symmetries of the relevant sites (Rancourt 1994a). In a series of papers, Rancourt and coworkers (Rancourt 1994a, 1994b; Rancourt et al. 1994) convincingly demonstrated that the QSD method performs better than the Lorentzian technique. Fits with Lorentzian doublets tend to overestimate the spectral backgrounds, put large wings or tails on the main absorption peaks, give unphysically large linewidths (Rancourt 1994a), and underestimate $Fe^{3+}/\Sigma Fe$ ratios by 1–2%. Thus, for comparison, we have chosen to model our Mössbauer spectra with the three different fitting techniques discussed above.

Samples were prepared for Mössbauer analysis by shredding them with a tweezer and spatula followed by grinding in a mortar and pestle under acetone to avoid oxidation. Approximately 10 mg of each sample, close to the thin absorber thickness as calculated by the method of Long et al. (1983), were then mixed with sugar and acetone and placed in the spectrometer sample holder, which is a plexiglas ring 3/8" in diameter. Although these precautions were undertaken to avoid the effects of preferred orientation, they were probably unnecessary because the crystals were all elongated, approximately equal mixture of fragments and fibers (Gunter et al. 2001). Spectra were acquired using a WEB Research Co. Mössbauer spectrometer in the Mineral Spectroscopy Laboratory at Mount Holyoke College. The instrument is equipped with a Janis Research Co. Model 850 closed-cycle He refrigerator capable of reaching temperatures from 12 to 700 K. Data were analyzed using the software package WMOSS by WEB Research Co., which has the capability to use Lorentzian or Voigt doublets or quadrupole splitting distributions (QSD).

Mössbauer spectra of all the samples are similar (Fig. 1). Results are given in Table 3 and include data from fits using Lorentzian, Voigt, and quadrupole splitting distribution models; a QSD fit is shown in Figure 2. At room temperature, each spectrum is composed of one (for Lorentzian and Voigt) or two (for QSD) $^{M}Fe^{3+}$ doublets/components and two $^{M}Fe^{2+}$ doublets/components. The two $^{M}Fe^{2+}$ components have similar isomer shifts (δ) of 1.12 mm/s but dramatically different values of quadrupole splitting (Δ =1.85 and 2.8 mm/s). Traditionally, these doublets have been assigned to $^{[M4]}Fe^{2+}$ and $^{[M1,M2,M3]}Fe^{2+}$, respectively (cf., Table 2), although some workers (Burns and Greaves 1971) have suggested that the lowest Δ doublet might be assigned to $^{M2}Fe^{2+}$.

One $^{M}Fe^{3+}$ feature, a sharp doublet with δ^* = 0.35 mm/s, is typical of octahedral Fe^{3+}. The second $^{M}Fe^{3+}$ component, which is present only in the QSD fits, is a broad feature with a similar isomer shift but very broad full widths at half maximum of the Gaussian. Based on these room-temperature spectra, it appeared that the latter Fe^{3+} component is a contribution from some impurity in the sample that was broadened by the onset of ferromagnetism (i.e., splitting into a sextet rather than a doublet). Because the majority of silicates undergo this transition at <100 K, this broadened feature strongly suggested the presence of an oxide phase as an impurity and made it clear that low-temperature spectra would be needed to accurately interpret the Mössbauer data from these samples. For this reason, low temperature spectra of the outcrop sample were acquired at 100 K and 12 K; the latter spectrum is shown in Figure 3.

Structure refinement

The X-ray diffraction data for WV no. 2* was collected with a Bruker/Siemens 3-circle platform SMART diffractometer (χ-axis fixed at 54.74°) at the University of Idaho. The frame data were acquired with the SMART software (SMART 1998) at 303(2) K using Mo$K\alpha$ radiation (λ = 0.71073 Å) from a normal-focus tube (see Table 4). Unit-cell constants were determined from 20

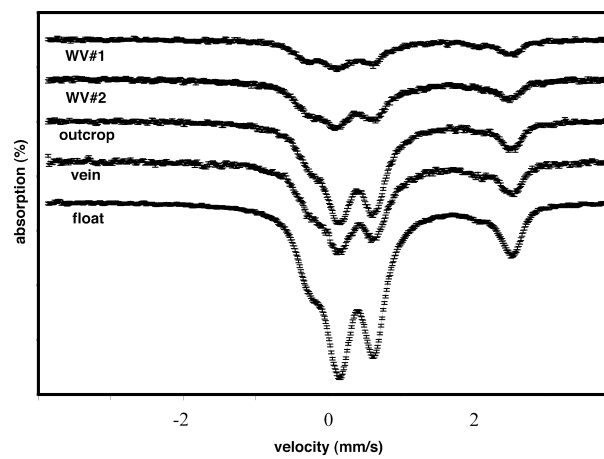

FIGURE 1. Room-temperature Mössbauer spectra of Libby amphiboles. Differences in absorption are due to variable Fe contents and sample thicknesses used; not enough sample was available to allow use of a consistent thickness.

TABLE 3. Results of Mössbauer analysis

			Fe^{3+}				Fe^{3+}				$^{[M2]}Fe^{2+}$ (M2)				$^{[M1+M3]}Fe^{2+}$					
Sample	Lineshape	χ2	Δ_0	σ_D	δ_0	Area	Δ_0	σ_D	δ_0	Area	Δ_0	σ_D	δ_0	Area	Δ_0	σ_D	δ_0	Area	Fe^{3+}_{raw}	Fe^{3+}_{cor}
WV	Lorentzian	0.56	0.53		0.37	61.5					1.84		1.15	7.6	2.83		1.13	33.6	59.9	55.0
no.1	Voigt	0.81	0.56		0.36	53.8					1.86		1.13	8.8	2.86		1.11	28.7	58.9	54.0
	QSD	0.55	0.51	0.47	0.38	29.2	0.53	2.66	0.35	30.8	1.90	0.00	1.13	7.0	2.86	0.53	1.13	29.1	62.4	57.7
WV	Lorentzian	1.49	0.58		0.37	59.3					1.15		0.77	12.2	2.80		1.07	32.0	57.3	52.4
no.2	Voigt	1.93	0.60		0.36	63.0					1.75		1.10	9.1	2.84		1.09	27.2	63.4	58.7
	QSD	0.60	0.50	0.50	0.40	31.1	0.54	3.07	0.34	44.4	2.11	0.87	1.04	10.8	2.78	0.51	1.15	23.2	68.9	64.5
Vein	Lorentzian	0.53	0.53		0.37	74.4					1.86		1.12	7.1	2.79		1.13	27.0	68.6	64.1
	Voigt	1.18	0.56		0.37	65.1					1.84		1.10	8.1	2.84		1.10	23.2	67.5	63.0
	QSD	0.42	0.49	0.51	0.40	37.1	0.38	2.88	0.33	35.4	1.93	0.62	1.10	10.0	2.85	0.51	1.15	22.7	68.9	64.5
Outcrop	Lorentzian	6.80	0.51		0.38	75.2					1.84		1.09	5.8	2.79		1.13	25.4	70.7	66.4
	Voigt	20.90	0.53		0.37	67.3					1.81		1.09	6.2	2.82		1.11	22.8	69.9	65.5
	QSD	1.58	0.49	0.40	0.39	42.0	0.37	2.57	0.29	32.7	1.95	0.73	1.09	7.0	2.77	0.46	1.14	20.2	73.3	69.3
Float	Lorentzian	0.74	0.51		0.38	79.0					1.82		1.13	3.4	2.78		1.13	22.6	75.2	71.4
	Voigt	2.39	0.53		0.37	69.8					1.82		1.10	5.2	2.83		1.10	19.7	73.7	69.6
	QSD	0.51	0.50	0.45	0.38	44.7	0.28	2.88	0.33	33.0	1.85	0.60	0.69	6.7	2.77	0.44	1.19	17.6	76.2	72.4

Notes: Values of δ_1 are 0.02 or less in all cases for fits using quadrupole splitting distributions. Γ is constrained to be equal to 0.20 mm/s, and h+/h– is constrained to be equal to 1. Symbols follow Rancourt and Ping (1991). Fe^{3+}_{raw} is the calculated peak area assigned to Fe^{3+}. Fe^{3+}_{cor} is the "true" corrected Fe^{3+} content based on a value of 1.22 for the recoil-free fraction correction in amphibole (cf., Dyar et al. 1993 for more information).

TABLE 4. Crystal structure collection methods and results

Temperature	303(2) K
Wavelength	0.71073 Å
Space group	*C*2/*m*
Unit cell dimensions	*a* = 9.8787(18) Å
	b = 18.024(3) Å
	c = 5.2875(10) Å
	β = 104.377(3)°
	Volume = 912.0(3) Å^3
Density (calculated)	3.013 Mg/m^3
Absorption coefficient	1.691 mm^{-1}
F(000)	823
Crystal size	0.39 × 0.14 × 0.11 mm^3
Diffractometer	Siemens SMART 1K
Theta range for data collection	2.41 to 24.99°.
Index ranges	$-9 \le h \le 11$, $-21 \le k \le 18$, $-6 \le l \le 6$
Reflections collected	2763
Independent reflections	834 (R_{int} = 0.0207)
Completeness to theta = 24.99°	99.4%
Absorption correction	Empirical*
Solution method	XS, Bruker SHELXTL v. 5.10
Refinement method	Full-matrix least-squares on F^2
Goodness-of-fit on F^2	1.048
Final *R* indices [$I > 2\sigma(I)$]	R_1 = 0.0335, wR_2 = 0.0994
R indices (all data)	R_1 = 0.0419, wR_2 = 0.1043
Largest diff. peak and hole	0.699 and –0.739 e.Å^{-3}

Note: $R_1 = \Sigma||F_o| - |F_c||/\Sigma|F_o|$; $wR_2 = \{\Sigma[w(F_o^2 - F_c^2)^2]/\Sigma[w(F_o^2)^2]\}^{1/2}$.
* SADABS (1999).

10 s frames. A complete hemisphere of data was scanned on omega (0.3° per scan) with a run time of 30 s per frame at the detector resolution of 512 × 512 pixels. A total of 1421 frames were collected in four sets, and a final set of 100 frames identical to the first 100 frames was also collected to determine crystal decay. The frames were then processed using the SAINTPlus software (SAINTPlus 1999) to give the raw data corrected for Lp/decay. The crystal used for the diffraction study showed no decomposition during data collection. The absorption correction was performed using the SADABS program (SADABS 1999). The structures were solved by direct method using SHELXS and refined by least squares method on F^2, using SHELXL; both programs are a part of SHELXTL v. 5.10 (SHELXTL 1998).

All non-hydrogen atoms were refined anisotropically. Site occupancies were initially assigned from diffraction data and then modeled until thermal parameters were approximately equal. Fractional positions and thermal parameters for the shared site atoms were also made equal. The A site (K, Na) is not completely filled (site occupancy factor of 0.48) and the low electron density and anisotropic refinement led to a prolate thermal displacement ellipsoid for this site. Ti was not included in the refinement because of its low concentration (0.01 apfu). The H atom (Table 5) was located on the difference map and refined with an occupancy equal to O3, which is a shared site atom. Atomic coordinates and temperature factors are given in Table 5, site occupancy data are given in Table 6, and selected bond lengths and the observed and calculated mean bond lengths for M1, M2, M3, and A are given in Table 7. The mean bond lengths are calculated based on the equation given in Hawthorne (1983). There is good agreement between the observed and calculated values, which helps validate our site assignments.

DISCUSSION

Low-temperature Mössbauer spectra

The low-temperature spectra proved to be the key to understanding the valence state of iron in these samples. A spectrum of the outcrop sample is shown in Figure 3. No sharp sextet is visible in this expanded-scale spectrum, indicating an absence of ferromagnetism. Thus, the broad Fe^{3+} component observed in the Libby amphibole spectra cannot be assigned to an impurity but must be contained within the amphibole crystal structure. This feature is consistent with the site occupancies calculated with Lorentzian and Voigt line shapes. For the "final" chemical compositions in Table 1, we used the area of the two Fe^{3+} components from the QSD fits, adjusted for the recoil-free fraction. Two possible explanations could explain the broad component observed in the QSD fits: (1) there is a distribution in crystal size, with some grains less than 1–10 μm wide (Gunter et al. 2001), or (2) the observed feature corresponds to isolated magnetic states for Fe^{3+}.

Effect of curve-fitting the line-shape for Mössbauer spectra

Because one of the goals of this project was to determine the Fe^{3+} contents of the Libby amphiboles, differences in $\%Fe^{3+}$ content that might result from fitting procedures were important. The far right-hand column of Table 3 shows the calculated Fe^{3+} content of the samples. The maximum variation due to the fitting model was observed for sample WV no. 2, which had a spread of 12.1% (absolute) in Fe^{3+} content. For all the

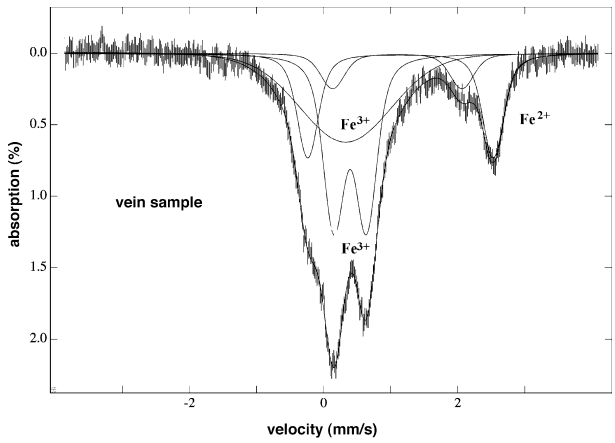

FIGURE 2. Mössbauer spectrum (dark curves showing noise) of the vein sample fitted using the quadrupole splitting distribution model (components shown as thin, smooth lines).

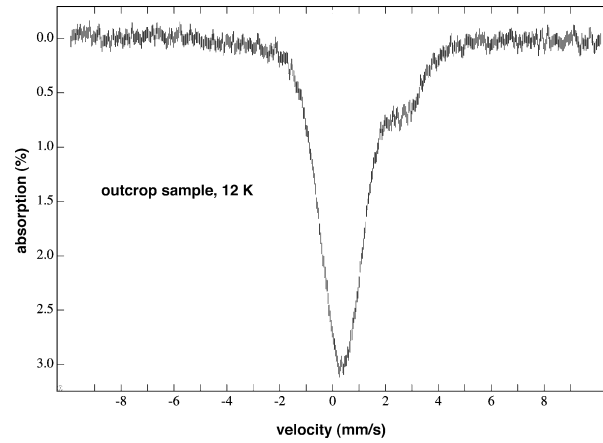

FIGURE 3. Low-temperature Mössbauer spectrum of the outcrop sample. Note the lack of features in the region from –10 to –3 and >4 mm/s, which indicates the absence of ferromagnetic species in this sample.

TABLE 5. Atomic coordinates and equivalent isotropic displacement parameters for WV no. 2*

Site	*x*/*a*	*y*/*b*	*z*/*c*	U_{eq}	U_{11}	U_{22}	U_{33}	U_{23}	U_{13}	U_{12}
T1	0.2791(1)	0.0848(1)	0.2960(2)	0.011(1)	0.015(1)	0.011(1)	0.008(1)	–0.001(1)	0.005(1)	0.000(1)
T2	0.2872(1)	0.1714(1)	0.8031(2)	0.011(1)	0.015(1)	0.012(1)	0.007(1)	0.000(1)	0.004(1)	–0.001(1)
M1	0.	0.0886(1)	0.5	0.009(1)	0.013(1)	0.009(1)	0.005(1)	0.	0.003(1)	0.
M2	0.	0.1796(1)	0.	0.010(1)	0.012(1)	0.011(1)	0.007(1)	0.	0.004(1)	0.
M3	0.	0.	0.	0.020(1)	0.026(1)	0.020(1)	0.016(1)	0.	0.007(1)	0.
M4	0.	0.2772(1)	0.5	0.018(1)	0.024(1)	0.016(1)	0.018(1)	0.	0.012(1)	0.
A	0.	0.5	0.	0.105(4)	0.127(8)	0.058(5)	0.188(11)	0.	0.147(8)	0.
O1	0.1113(2)	0.0865(1)	0.2166(4)	0.013(1)	0.017(1)	0.013(1)	0.008(1)	–0.001(1)	0.004(1)	–0.001(1)
O2	0.1186(2)	0.1702(1)	0.7269(4)	0.014(1)	0.017(1)	0.015(1)	0.011(1)	–0.001(1)	0.005(1)	–0.001(1)
O3	0.1081(3)	0.	0.7138(6)	0.014(1)	0.018(2)	0.016(2)	0.010(2)	0.	0.006(1)	0.
O4	0.3634(2)	0.2487(1)	0.7956(4)	0.015(1)	0.020(1)	0.015(1)	0.009(1)	–0.001(1)	0.005(1)	–0.004(1)
O5	0.3459(2)	0.1315(1)	0.0922(4)	0.015(1)	0.018(1)	0.018(1)	0.010(1)	0.004(1)	0.005(1)	0.000(1)
O6	0.3419(2)	0.1182(1)	0.5877(4)	0.014(1)	0.017(1)	0.015(1)	0.011(1)	–0.002(1)	0.004(1)	–0.001(1)
O7	0.3364(3)	0.	0.2935(6)	0.016(1)	0.013(2)	0.016(2)	0.016(2)	0.	0.004(1)	0.
H	0.2148	0.	0.7750	0.030(20)	nd	nd	nd	nd	nd	nd

Note: U_{eq} is defined as one-third of the trace of the orthogonalized U_{ij} tensor, and anisotropic displacement parameters, where the anisotropic displacement factor exponent takes the form: $-2\pi 2[h2\,a^{*}2U_{11} + \ldots + 2\,h\,k\,a^{*}\,b^{*}\,U_{12}]$.

TABLE 6. Cation site occupancies determined by X-ray diffraction (XRD), Mössbauer spectroscopy (Möss), and EMPA for WV no. 2*

	Si	Al	Mg	Fe Fe^{3+} / Fe^{2+}*	Mn	Ca	Na	K	Site sum
T	7.96	0.04							8.00
M1		0.02	1.98						2.00
M2			1.64	0.36 0.34 / 0.06					2.00
M3			0.84	0.16 0.00 / 0.13					1.00
M4					0.04	1.12	0.84		2.00
A							0.28	0.20	0.48
Sums from XRD & Möss		0.06	4.46	0.52 0.34 / 0.19	0.04	1.12	1.12	0.20	
Sums from EMPA	7.96	0.06	4.46	0.52 0.34 / 0.19	0.04	1.12	1.17	0.19	

* Fe^{3+} / Fe^{2+} site occupancies determined by Mössbauer spectroscopy.

other samples, the spread was less than 3% absolute. This result suggests that, in this suite of samples, the measured Fe^{3+} content is not model-dependent. As predicted by Rancourt (1994a, b) and Rancourt et al. (1994), the QSD model does tend to give slightly higher Fe^{3+} contents than the older models. This result suggests that Mössbauer analyses reported in earlier studies need not be discarded, but should definitely be reported with slightly larger errors than previously reported.

Site occupancies of Fe and other atoms

In this study, two different techniques were used to evaluate the occupancies of the Fe sites: Mössbauer spectroscopy

TABLE 7. Selected bond distances, observed mean bond distances, and calculated mean bond distances for M1, M2, and M3-sites for WV no. 2*

Bonds	Distances (Å)	Bonds	Distances (Å)
T1-O1	1.606(2)		
T1-O5	1.630(2)		
T1-O6	1.627(2)	M3-O1 ×4	2.080(2)
T1-O7	1.631(2)	M3-O3 ×2	2.058(3)
$<T1-O>_{obs}$	1.624	$<M3-O>_{obs}$	2.073
		$<M3-O>_{calc}$	2.068
T2-O2	1.613(3)		
T2-O4	1.589(3)		
T2-O5	1.658(2)	M4-O2 ×2	2.415(3)
T2-O6	1.679(2)	M4-O4 ×2	2.351(2)
$<T2-O>_{obs}$	1.635	M4-O5 ×2	2.836(2)
		M4-O6 ×2	2.564(2)
M1-O1 ×2	2.067(2)	$<M4-O>_{obs}$	2.542
M1-O2 ×2	2.068(2)		
M1-O3 ×2	2.091(2)		
$<M1-O>_{obs}$	2.075		
$<M1-O>_{calc}$	2.076	A-O5 ×4	2.923(2)
		A-O6 ×4	3.167(2)
M2-O1 ×2	2.171(2)	A-O7 ×2	2.503(3)
M2-O2 ×2	2.080(2)	$<A-O>_{obs}$	2.937
M2-O4 ×2	1.983(2)		
$<M2-O>_{obs}$	2.078		
$<M2-O>_{calc}$	2.069		

and single crystal X-ray diffraction, for which we obtained EMPA data from the crystal used for structure analysis. In order to use the Mössbauer effect to determine site occupancies, it is necessary to use the QSD model. Rancourt (1994a) showed the inadequacy of Lorentzian doublets for fitting spectra of naturally occurring mica samples. Rancourt (1994b) further noted that "fitting with Lorentzian doublets can at best give phenomenological characterizations of spectra, whereas QSDs are true physical quantities amenable to theoretical calculations and crystal chemical interpretation." He showed that Mössbauer spectra of 2:1 layer silicates cannot resolve the octahedral Fe^{2+} cis (M2) and trans (M1) sites, and he supported his contention that "interpretations in terms of octahedral Fe^{2+} cis and trans sites are incorrect and cannot be used to even estimate cis/trans site population ratios." Rancourt (1994b) then concluded by strongly stating that "we recommend that spectroscopists now break from this admittedly compelling interpretation (of Lorentzian line shape doublets assigned to cis and trans sites) to consider the QSD."

A similar physical situation exists for the amphibole group minerals, which can be expected to have heterogeneous configurations of next nearest neighbor atoms because they are compositionally so variable and complex. Thus, it is important to consider whether the traditional assignments of amphibole Mössbauer spectra to Fe at specific sites in the structure are robust. Several studies have compared the results of Mössbauer site assignments (calculated using Lorentzian line-shapes) to the results of single-crystal X-ray diffraction (XRD). For example, Evans et al. (2001) showed strong agreement between the Mössbauer data of Seifert (1978) and their own single-crystal XRD results for two-doublet Lorentzian fits to Fe^{2+} doublets assigned to M4 and M1-3. A comparison of XRD and Mössbauer data from a suite of cummingtonite samples was carried out by Grant (1995). He suggested that excellent agreement between XRD and Mössbauer site occupancies in amphibole can be obtained if thickness and recoil-free fraction effects are considered, along with use of Voigt or QSD lineshapes.

There is consistency between our Mössbauer and XRD results. As shown in Table 3, 64.5% of the total Fe is Fe^{3+}, or 0.34 apfu, and 35.5%, or 0.19 apfu, is Fe^{2+} (Table 1, WV no. 2*). The Fe^{2+} doublet with the lowest quadrupole splitting is assigned to $^{M2}Fe^{2+}$, following the convention of Burns and Greaves (1971), while the other Fe^{2+} doublet represents an unresolvable combination of $^{M1+M3}Fe^{2+}$. Because the site refinement shows only Mg and Al at the M1 site, we conclude that this doublet here represents only $^{M3}Fe^{2+}$. Thus, of the Fe^{2+}, 31.8% or 0.06 apfu is at M2, and 68.2% or 0.13 apfu is at M3, compared to 0.16 apfu Fe by XRD (Table 6). Overall, there is excellent agreement between the two techniques, similar to what has been observed in previous studies. Therefore, for amphibole group minerals (unlike the situation for micas) it is probably still appropriate to use Mössbauer fits to assign site occupancies for Fe.

All the cation assignments, including Fe, are listed in Table 6. In addition to the excellent agreement between the Mössbauer and XRD results for Fe, there is also excellent agreement between the XRD data and the EMPA data as revealed by the "sums" row in Table 6. The site assignment method from Leake et al. (1997) cannot discriminate between M1, M2, and M3 when treating all of them as "C" in the general formula $A\,B_2\,C_5\,T_8\,O_{22}\,(O,OH,F,Cl)_2$, but when the contents of "C" (Table 1), as assigned according to the method of Leake et al. (1997), are compared to the summed contents of M1, M2, and M3 in Table 6, they are also in excellent agreement. One reason for the agreement between XRD and EMPA results is that both sets of data were collected from the same single crystal, which is often not the case. Frequently one will assume that chemical results will be the same for crystals "out-of-the-same-bottle." As shown in Table 1, this is not the case; there is a significant difference in composition between WV no. 2 and WV no. 2*. Also, as stated above, significantly different compositions were found in the suite of three samples from Libby. Significant variation between crystals from the same samples was also observed. For example, for the 16 different crystals analyzed for the float sample, the apfu values ranged from 1.03 to 1.42 for Ca and 0.78 to 1.18 for Na. While some of this is experimental error in the EMPA data, some of the variation could represent compositional differences.

Libby amphiboles: chemical formulas, species names, and implications for asbestos classification

To date there have been six published chemical analyses of single crystals of amphibole from the former vermiculite mine near Libby (summarized in Table 1). Based on the site assignments in Table 1 and the classification scheme of Leake et al. (1997), all of these samples belong to the sodic-calcic group of amphiboles. At the species level, two of these samples are classified as richterite (A-site occupancy ≥0.5) and four as winchite (A-site occupancy <0.5). Interestingly, WV no. 2 and WV no. 2* might be classified as winchite and richterite, respectively, based on compositional determinations made by two different research groups. Our chemical analysis was not obtained from the same single crystal as that of Wylie and Verkouteren (2000),

but rather from a crystal from the same bulk sample. Of course, some chemical variation within these natural samples might be expected. Moreover, of the 25 analyses of WV no. 2*, which were averaged in Table 1 to arrive at the final formula, 11 had A-site occupancies less than 0.5. This would define the sample as a winchite. Thus, this sample resides compositionally at the boundary between these two species. In addition, four bulk-sample analyses of Libby amphiboles have been published to date: a wet chemical analysis by Larsen (1942) showed richterite; three bulk-sample XRF analyses by Gunter et al. (2001) on the same suite of samples used in this study (vein, outcrop, float) all showed winchites. The XRF analysis of bulk samples (Gunter et al. 2001) yielded slightly higher Al and K concentrations and lower Ca and Mg concentrations than the single crystals studied here. This result probably reflects microscopic impurities of sheet silicates in the bulk samples.

Historically, the amphiboles at Libby were called tremolite or actinolite by the majority of workers in the health fields (McDonald et al. 1986a, 1986b; Amandus and Wheeler 1987; Amandus et al. 1987a, 1987b; McDonald et al. 1988; Weill et al. 1990), regulatory agencies (USEPA 2000), and by the media. Our data and those of Wylie and Verkouteren (2000) suggest instead that these amphiboles are dominantly winchites and richterites. There is no doubt that it is important for mineralogists and petrologists to set criteria for precise definition of mineral species names, as was done by Leake et al. (1997). Others in the sciences and regulatory fields must use these names to avoid confusion. However, we must realize the limitations to placing a name on a mineral that occurs in a solid solution series. For instance, using winchite and richterite as examples, a winchite with an A-site occupancy of 0.49 would be more similar (i.e., its physical, structural, and chemical properties) to a richterite with an A-site occupancy of 0.50 than it would to a winchite with an A-site occupancy of 0.1, yet the mineral name would be different for the first set and the same for the second.

ACKNOWLEDGMENTS

We thank S. Hale for assistance with the Mössbauer experiments, and T. Kent for advice on fitting and interpreting quadrupole splitting distributions. We are especially thankful to A. Wylie and J. Verkouteren for sharing their samples with us and to M. Ross and an anonymous reviewer for very helpful comments on this article. This work was supported by NSF grants EAR-9811870, EAR-9909587, and EAR-9806182.

REFERENCES CITED

Amandus, H.E. and Wheeler, R. (1987) The morbidity and mortality of vermiculite miners and millers exposed to tremolite-actinolite: Part II. Mortality. American Journal of Industrial Medicine, 11, 15–26.

Amandus, H.E., Wheeler, R., Jankovic, J., and Tucker, J. (1987a) The morbidity and mortality of vermiculite miners and millers exposed to tremolite-actinolite: Part I. Exposure estimates. American Journal of Industrial Medicine, 11, 1–14.

Amandus, H.E., Althouse, R., Morgan, W.K.C., Sargent, E.N., and Jones, R. (1987b) The morbidity and mortality of vermiculite miners and millers exposed to tremolite-actinolite: Part III. Radiographic findings. American Journal of Industrial Medicine, 11, 27–37.

Bancroft, G.M. and Brown, J.R. (1975) A Mössbauer study of coexisting hornblendes and biotites: quantitative Fe^{3+}/Fe^{2+} ratios. American Mineralogist, 60, 265–272.

Bancroft, G.M. and Burns, R.G. (1969) Mössbauer and absorption spectral study of alkali amphiboles. Mineralogical Society of American Special Paper, 2, 137–150.

Bancroft, G.M., Burns, R.G., and Maddock, A.G. (1967a) Determination of the cation distribution in the cummingtonite-grunerite series by Mössbauer spectra. American Mineralogist, 52, 1009–1026.

Bancroft, G.M., Maddock, A.G., and Burns, R.G. (1967b) Applications of the Mössbauer effect to silicate mineralogy - I. Iron silicates of known crystal structure. Geochimica et Cosmochimica Acta, 31, 2219–2246.

Bandli, B.R. (2002) Characterization of amphibole and amphibole-asbestos from the former vermiculite mine at Libby, Montana. M.S. Thesis, University of Idaho.

Boettcher, A.L. (1966) Vermiculite, hydrobiotite, and biotite in the Rainy Creek igneous complex near Libby, Montana. Clay Minerals, 6, 283–296.

——— (1967) The Rainy Creek alkaline-utramafic igneous complex near Libby, Montana. I: Ultramafic rocks and fenite. Journal of Geology, 75, 526–553.

Burns, R.G. and Greaves, C. (1971) Correlations of infrared and Mössbauer site population measurements of actinolites. American Mineralogist, 56, 2010–2033.

Dyar, M.D., Mackwell, S.M., McGuire, A.V., Cross, L.R., and Robertson, J.D. (1993) Crystal chemistry of Fe^{3+} and H^+ in mantle kaersutite: Implications for mantle metasomatism. American Mineralogist, 78, 968–979.

Ernst, W.G. and Wai, C.M. (1970) Mössbauer, infrared, X-ray and optical study of cation ordering and dehydrogenation in natural and heat-treated sodic amphiboles. American Mineralogist, 55, 1226–1258.

Evans, B.W., Ghiorso, M.S., Yang, H., and Medenbach, O. (2001) Thermodynamics of the amphiboles: Anthophyllite-ferroanthophyllite and the ortho-clino phase loop. American Mineralogist, 86, 640–651.

Ghose, S., Kersten, M., Langer, K., Rossi, G., and Ungaretti, L. (1986) Crystal field spectra and Jahn Teller effect of Mn^{3+} in clinopyroxene and clinoamphiboles from India. Physics and Chemistry of Minerals, 13, 291–305.

Goldman, D.S. (1979) A reevaluation of the Mössbauer spectroscopy of calcic amphiboles. American Mineralogist, 64, 109–118.

Goodman, B.A. and Wilson, M.J. (1976) A Mössbauer study of the weathering of hornblende. Clay Minerals, 11, 153–163.

Grant, C.G. (1995) Sources of Experimental and Analytical Error in Measurements of the Mössbauer Effect in Amphibole. Ph.D. thesis, University of Oregon, 217 pp.

Gunter, M.E., Brown, B.M., Bandli, B.R., and Dyar, M.D. (2001) Amphibole-asbestos, vermiculite mining, and Libby, Montana: What's in a name? Eleventh Annual Goldschmidt Conference, Hot Springs, Virginia.

Hawthorne, F.C. (1983) The crystal chemistry of amphiboles. Canadian Mineralogist, 21, 173–480.

Larsen, E.S. (1942) Alkalic rocks of Iron Hill, Gunnison County, Colorado. U.S. Geological Survey Professional Paper, 197-A, 64.

Leake, B.E., Woolley, A.R., Arps, C.E.S., Birch, W.D., Gilbert, M.C., Grice, J.D., Hawthorne, F.C., Kato, A., Kisch, H.J., Krivovichev, V.G., Linthout, K., Laird, J., Mandarino, J.A., Maresch, W.V., Nickel, E.H., Rock, N.M.S., Schumacher, J.C., Smith, D.C., Stephenson, N.C.N., Ungaretti, L., Whittaker, E.J.W., and Youzhi, G. (1997) Nomenclature of the amphiboles: Report of the subcommittee on amphiboles of the International Mineralogical Association, Commission on New Minerals and Mineral Names. Canadian Mineralogist, 35, 219–246.

Litvin, A.L., Michnik, T.L., Ostapenko, S.S., and Pol'shin, E.V. (1973) X-ray and Mössbauer investigations of cation distribution in catophorite (taramite). Geologicheskiy Zhurnal, 33, 49–56.

Long, G.J., Cranshaw, T.E., and Longworth, G. (1983) The ideal Mössbauer effect absorber thicknesses. Mössbauer Effect Reference Data Journal, 6, 42–49.

Luys, M.-J., Gilbert, L.D.-R., Adams, F., and Vansant, E.F. (1983) Cation site populations in amphibole asbestos. Journal of the Chemical Society, Faraday Transactions 1, 79, 1451–1459.

McDonald, J.C., McDonald, A.D., Armstrong, B., and Sebastien, P. (1986a) Cohort study of the mortality of vermiculite miners exposed to tremolite. British Journal of Industrial Medicine, 43, 436–444.

McDonald, J.C., Sebastien, P., and Armstrong, B. (1986b) Radiological survey of past and present vermiculite miners exposed to tremolite. British Journal of Industrial Medicine, 43, 445–449.

McDonald, J.C., McDonald, A.D., Sebastien, P., and Moy, K. (1988) Health of vermiculite miners exposed to trace amounts of fibrous tremolite. British Journal of Industrial Medicine, 45, 630–634.

Nysten, P. and Skogby, H. (1994) Manganese ferro-ferri-winchite from Harstigen, Filipstad, central Sweden. Mineralogical Magazine, 58, 168–172.

Ping, J.Y., Rancourt, D.G., and Stadnik, Z.M. (1991) Voigt-based methods for arbitrary shape quadrupole splitting distributions (QSD's) applied to quasi-crystals. Hyperfine Interactions, 69, 493–496.

Rancourt, D.G. (1994a) Mössbauer spectroscopy of minerals I. Inadequacy of Lorentzian-line doublets in fitting spectra arising from quadrupole splitting distributions. Physics and Chemistry of Minerals, 21, 244–249.

——— (1994b) Mössbauer spectroscopy of minerals II. Problem of resolving cis and trans octahedral Fe^{2+} sites. Physics and Chemistry of Minerals, 21, 250–257.

Rancourt, D.G., Ping, J.Y., and Berman, R.G. (1994) Mössbauer spectroscopy of minerals III. Octahedral-site Fe^{2+} quadrupole splitting distributions in the phlogopite-annite series. Physics and Chemistry of Minerals, 21, 258–267.

SADABS (1999) Version 2.01, Bruker/Siemens Area Detector Absorption Program, Bruker AXS, Madison, Wisconsin.

SAINTPlus (1999) Version 6.02, Data Reduction and Correction Program, Bruker AXS, Madison, Wisconsin.

Schmidbauer, E., Kunzmann, Th., Fehr, Th., and Hochleitner, R. (2000) Electrical

resistivity and ^{57}Fe Mössbauer spectra of calcic amphiboles. Physics and Chemistry of Minerals, 27, 347–356.
Seifert, F.A. (1978) Equilibrium Mg-Fe^{2+} cation distribution in anthophyllite. American Journal of Science, 278, 1323–1333.
Semet, M. (1973) A crystal-chemical study of synthetic magnesio-hastingite. American Mineralogist, 58, 480–494.
SHELXTL (1998) Version 5.10, Structure Determination Software Suite, Bruker AXS, Madison, Wisconsin.
SMART (1998) Version 5.059, Bruker Molecular Analysis Research Tool, Bruker AXS, Madison, Wisconsin.
Sokolova, E.V., Kabalov, Y.K., McCammon, C., Schneider, J., and Konev, A.A. (2000) Cation partitioning in an unusual strontian potassicrichterite from Siberia: Rietveld structure refinement and Mössbauer spectroscopy. Mineralogical Magazine, 64, 19–23.
Sokolova, E.V., Hawthorne, F.C., Gorbatova, V., McCammon, C., and Schneider, J. (2001) Ferrian winchite from the Ilmen Mountains, Southern Urals, Russia and some problems with the current scheme of nomenclature. Canadian Mineralogist, 39, 171–177.
United States Environmental Protection Agency (2000) Sampling and analysis of consumer garden products that contain vermiculite. Report 2001-S-7, United States Environmental Protection Agency, Washington, D.C.
United States Environmental Protection Agency (2001) EPA's actions concerning asbestos-contaminated vermiculite in Libby, Montana. EPA 744-R-00-010, United States Environmental Protection Agency, Washington, D.C.
Vanderberghe, R.E., DeGrave, E., and de Bakker, P.M.A. (1994) On the methodology of the analysis of Mössbauer spectra. Hyperfine Interactions, 83, 29–49.
Virgo, D. (1972) Preliminary fitting of ^{57}Fe Mössbauer spectra of synthetic Mg-Fe richterites. Year Book, Carnegie Institution of Washington, 71, 513–516.
Voigt, W. (1912) Über das Gesetz der Intensitätsverteilung innerhalb der Linien eines Gasspektrums. Sitzungsberichte der mathematisch-physikalischen. Klasses der Königlich Bayerischen Akademie der Wissenschaften, 603–620.
Weill, H., Abraham, J.L., Balmes, J.R., Case, B., Chrug, A., Hughes, J., Schenker, M., and Sebastien, P. (1990) Health effects of tremolite. American Review of Respiratory Diseases, 142, 1453–1458.
Wylie, A.G. and Huggins, C.W. (1980) Characteristics of a potassian winchite-asbestos from the Allamorre talc-district, Texas. Canadian Mineralogist, 18, 101–107.
Wylie, A.G. and Verkouteren, J.R. (2000) Amphibole asbestos from Libby, Montana: Aspects of nomenclature. American Mineralogist, 85, 1540–1542.

MANUSCRIPT RECEIVED MARCH 4, 2003
MANUSCRIPT ACCEPTED APRIL 14, 2003
MANUSCRIPT HANDLED BY JILL PASTERIS